

Time-frequency analysis of magnetotelluric data

I. J. Chant and L. M. Hastie

Physics Department, University of Queensland, Queensland 4072, Australia

Accepted 1992 May 25. Received 1992 May 11; in original form 1991 October 10

SUMMARY

The natural signal magnetotelluric (MT) and audiomagnetotelluric (AMT) geophysical prospecting methods utilize the spectra of associated time-varying horizontal electric and magnetic fields at the Earth's surface to determine a frequency-dependent impedance tensor. Most present methods of analysis determine the spectra using variations on the Fourier transform and therefore must assume either that the signals under analysis are stationary over the record length or that any distortion in the spectral estimations due to non-stationarity will occur in an equivalent manner in the spectra of both the electric and magnetic fields and thus not effect the impedance estimates. We use time-frequency distribution (TFD) analysis techniques to show that this is not the case, and that the impedance tensor is affected by non-stationary source field fluctuations. We further show that TFD analysis techniques can be used to overcome these problems and obtain stable and reliable estimates of the impedance tensor. These techniques are compared with previous techniques by using a standard data set (EMSLAB).

Key words: EMSLAB, magnetotellurics, non-stationarity, time frequency.

INTRODUCTION

In magnetotelluric data analysis the spectra of time-varying electric and magnetic field measurements at the Earth's surface are used to obtain the impedance of the ground as a function of frequency. These fields are induced in the Earth by electromagnetic waves propagating in the Earth-ionosphere waveguide. These electromagnetic fields can be naturally produced by ionospheric, magnetospheric or atmospheric events. When the sources of these signals are far enough removed from the sounding site the waveforms may be analysed as plane waves vertically incident on the Earth's surface. The plane waves induce current flows in the Earth which give rise to secondary fields at the surface. By measuring the horizontal electric and magnetic fields as they vary with time at the Earth's surface we can calculate a tensor impedance (equation 1) for the site as a function of frequency (Vozoff 1972).

$$\begin{pmatrix} E_x \\ E_y \end{pmatrix} = \begin{pmatrix} Z_{xx} & Z_{xy} \\ Z_{yx} & Z_{yy} \end{pmatrix} \begin{pmatrix} B_x \\ B_y \end{pmatrix}. \quad (1)$$

\mathbf{Z} is the MT impedance tensor defined by Berdichevsky (1960, 1964) and Tikonov & Berdichevsky (1966). The components of the impedance tensor are referred to as polarizations, the E -polarization refers to the xy tensor component and the H -polarization refers to the yx tensor component (Reddy & Rankin 1975).

In practice these measured field strengths contain contributions from many sources, not all of which obey the

assumptions necessary for MT analysis. For instance the data may be contaminated by local natural or artificial noise sources (Dekker & Hastie 1981; Goubau, Gamble & Clarke 1978). High power, non-stationary transients, which cause serious bias when standard processing methods are used, may also be present. Such sources are difficult to remove from data since, though transient, they are usually highly coherent. Some attempt has been made to remove such contamination by data editing (Jones & Jödicke 1984), but this method cannot attack the problem of less energetic contamination which is not readily separated from the desirable signal.

To date, attempts to remove contamination using signal processing techniques have usually relied on coherence to establish data quality (Jones 1981). This can be self-defeating when coherent noise is present and may bias the data as we will demonstrate later. Another type of analysis, called remote reference, uses extra components measured simultaneously at a spatially separated location, in an attempt to reject local contamination (Chave & Thompson 1989; Chave, Thompson & Ander 1987). All these methods use stationary spectral analysis methods such as the Fourier transform to estimate the spectrum. This implies that the time series being analysed are reasonably self-stationary.

MT SPECTRAL ANALYSIS TECHNIQUES

Any time series or sequences can be processed using a Fourier transform and the decomposition in terms of

sinusoids will invert to give the original series or sequence. This is a mathematical operation, and there are many other possible decompositions that can be used. The reason why the Fourier transform is generally favoured over other possible mathematical decompositions, is that often the energy at any frequency interval of the Fourier power spectrum is directly related to the energy in the same frequency interval for the signal source. For this to be true, certain assumptions must be made about the nature of the time-series data, and one of the important assumptions is that the power distribution in the signal does not vary with time. This condition is called stationarity, or self-stationarity when referring to a finite length time series.

The effect of non-stationarity can easily be demonstrated by the use of a simple deterministic non-stationary signal such as the linear chirps shown in Fig. 1. The chirps have energy in only one frequency at a time and the energy is constant and identical for both signals. The Fourier transform representation indicates that the broader bandwidth chirp signal has less energy present at any time and in any frequency than the smaller bandwidth chirp, and the signal power is present in all frequencies in the bandwidth

throughout the recording time. This is obviously a very poor representation of the original signal. Therefore a non-stationary representation should be used which will produce a proper energy estimate at a single frequency component which varies with time according to the chirp law.

However, in MT analysis, one is generally only interested in the ratio of the power in the electric and magnetic field components, so there has been an implicit assumption that, if any non-stationary distortion is present in a signal, it will be present to the same degree in both related field components. Thus the input impedances calculated from the data would remain valid in spite of the non-stationarity of the signal. For a regular sort of non-stationarity such as the chirp shown, this would be true provided the signal-to-noise ratio is high. However MT signals are generally due to multiple sources that could stop and start quite abruptly, so there is no guarantee that that the ratio will remain so well behaved. This is particularly true of the phase estimations, which are very unstable in the presence of non-stationary signal components.

In order to test this hypothesis of impedance invariance to signal non-stationarity, non-stationary spectral estimators

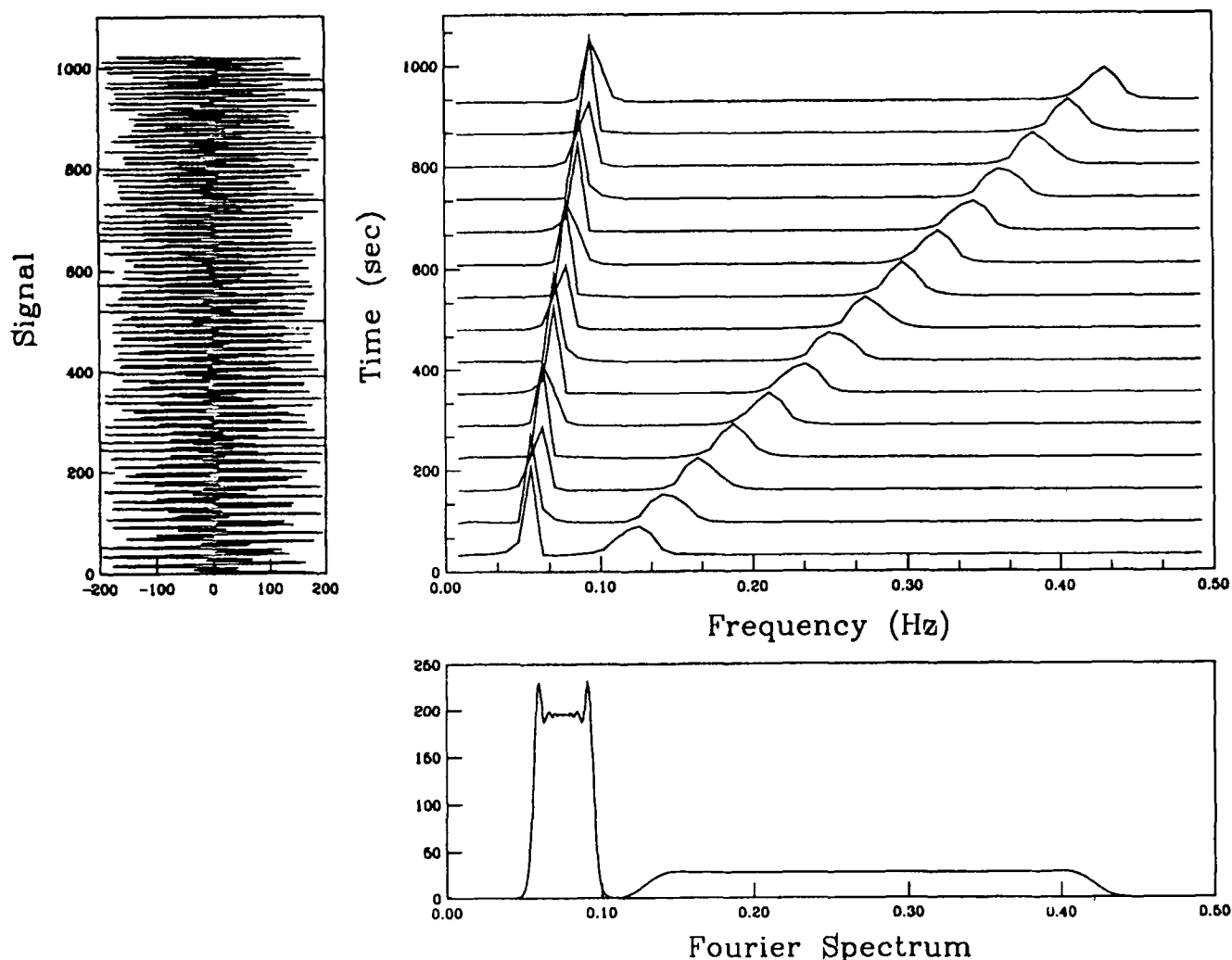


Figure 1. A plot comparing the Fourier spectrum and STFT evulsive spectrum of a two-component FM signal, showing the loss of information in the Fourier spectrum.

were used to provide time-varying (evolutive) spectral estimates for the signals. These were found to be highly non-stationary, though the power spectral estimates were found to conform to a χ^2 distribution as do the power estimations derived using the Fourier transform (Chave *et al.* 1987). In fact, there was a negligible stationary component. These spectra were used to calculate the time-varying (evolutive) impedance estimates, which should then conform to a log-normal distribution as they are the division of two χ^2 distributions (Soong 1981). If the assumption that non-stationarity did not effect impedance estimates was correct then the impedance estimates of any frequency should be constant with time except for some Gaussian-type noise. In fact the evolutive impedances were found to show significant diversions from the constant impedance which could be directly associated with non-stationary signals, as can be seen by inspection of Figs 2 and 3.

Thus there exists a very strong case for using the evolutive impedances to estimate the stationary impedance over each frequency interval, and use these as the basic MT impedance estimates. Of course, if any stationary noise source is present, this will still contaminate the stationary estimates obtained by the above procedure. However the non-stationary biases will have been minimized and other existing procedures, such as remote reference, can be used

to minimize specific sources of stationary noise. It should be noted that stationarity is an essential assumption not just for the Fourier transform, but for most spectral transforms in common use including all those compared in Jones *et al.* (1989).

In this paper we use time-frequency signal processing methods, which are robust to non-stationarity, to calculate stationary MT impedance estimates. We further show that non-stationarity adversely effects the impedance estimations made by conventional stationary analysis methods and also that analysis based primarily on selection of data by stationary coherency of signals is likely to result in biased impedance estimations.

NON-STATIONARITY TESTS

It can be shown by application of non-stationary tests (Bendat & Piersol 1971, p. 234–237) that the MT data to be analysed in this paper is *strongly* non-stationary. These tests examine the stability of the signal statistics as they vary with time, but do not require contiguous data. To test a signal for stationarity, the combined sample length must be long enough to be a representative segment of the process as well as being long compared to the lowest frequency content. It is reasonable to assume that the non-stationarity will be evident in the mean square statistic of the data.

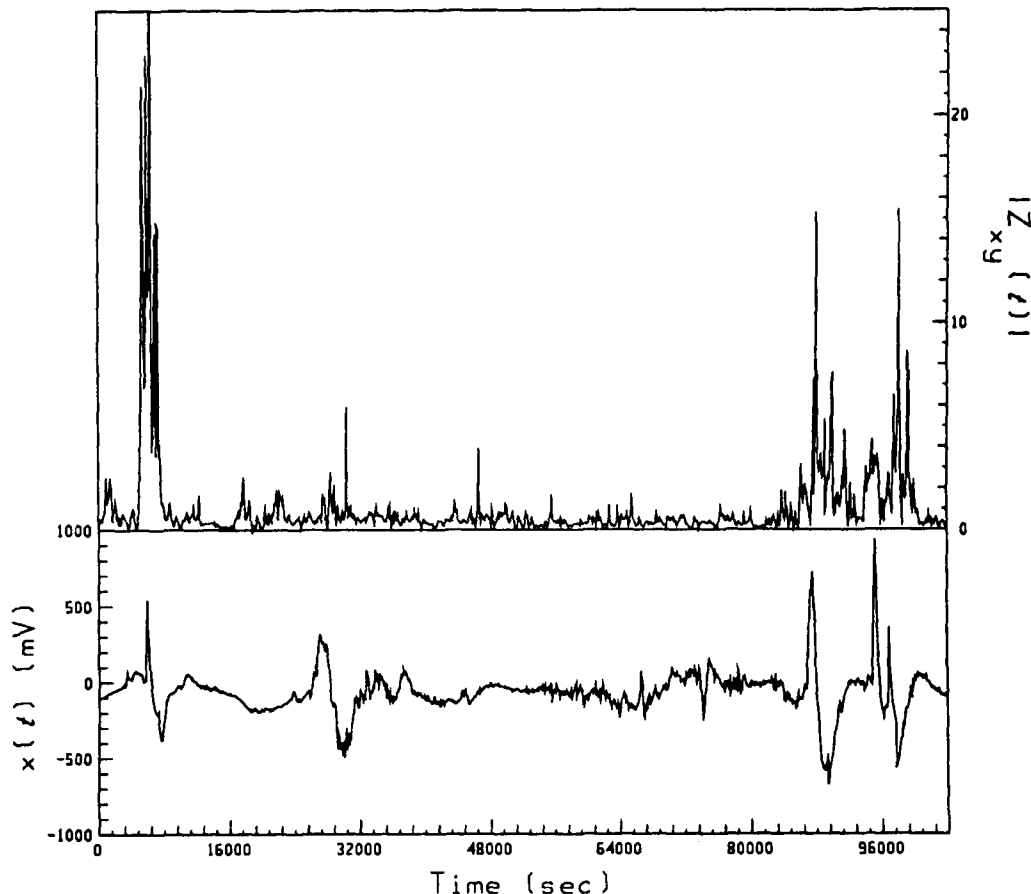


Figure 2. An example of the temporal variation in impedance at 4.39×10^{-4} Hz, with the signal plotted on the same time-scale for comparison. The temporal variation was found using the cone kernel time-frequency distribution. Note that the obviously highly non-stationary transients coincide with major variations in impedance.

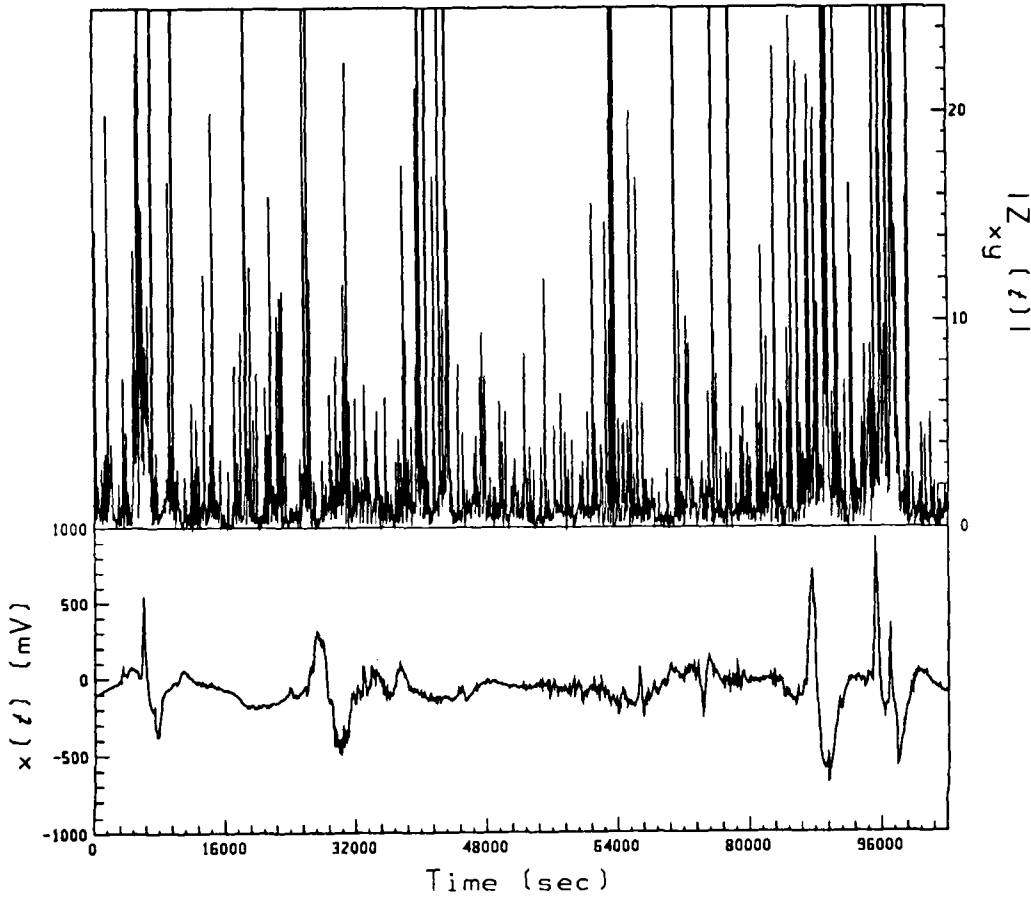


Figure 3. An example of the temporal variation in impedance at 4.39×10^{-4} Hz, with the signal plotted on the same time-scale for comparison. The temporal variation was found using the STFT time-frequency distribution. Note the much greater noise level than that exhibited by the cone kernel impedances.

To determine the stationarity of a signal, we first compute the mean squares of multiple discrete equal-length segments. With the mean square estimators arranged in temporal order we then apply a non-parametric test statistic such as the run test (Bendat & Piersol 1971, p. 156) to determine whether the estimators are part of the same population. On the EMSLAB data this test returned a figure in excess of 99 per cent certainty that all the data records were non-stationary, demonstrating the necessity for a time-frequency analysis of MT data.

TIME-FREQUENCY DISTRIBUTIONS

When a signal is found to be time varying, or non-stationary, then accurate spectral analysis cannot be accomplished with classical time-domain representations such as correlation methods or frequency-domain representations based on the Fourier transform. For non-stationary signals, the concept of time-frequency distributions (TFDs) has been developed as an extension of classical Fourier analysis, in order to provide a joint function of time and frequency that will describe the energy density of a signal simultaneously in time and frequency (Boashash 1991; Lovell 1991). This is sometimes called the evolutive spectrum since it shows how the spectrum evolves with time. Fig. 1 shows the evolutive spectrum of two FM chirp functions, together with the corresponding time series and

Fourier transform spectrum (in order to highlight the lack of important information in the Fourier spectrum) for representing time-varying signals. As yet, no universally effective TFD has been found, although some of the existing functions are very useful in non-stationary analysis.

All popular TFDs are members of Cohen's general class (Cohen 1967), which is defined for analytic signals by

$$\mathcal{P}(t, f) = \int_{-\infty}^{\infty} \int_{-\infty}^{\infty} \int_{-\infty}^{\infty} e^{j2\pi(\nu\mu - \tau f - \nu t)} f(\nu, \tau) z(\mu + \tau/2) \times z^*(\mu - \tau/2) d\mu d\tau d\nu, \quad (2)$$

where $f(\nu, \tau)$ is the Cohen kernel function, $z = x + j\mathcal{H}(x)$, is the analytic signal corresponding to real signal $x(t)$ and $\mathcal{H}(x)$ is the Hilbert transform of x . j is the $\sqrt{-1}$.

This is more usefully expressed as,

$$\mathcal{P}(t, f) = \mathcal{F}_{t \rightarrow f} \left\{ \Phi(-t, \tau) *_{(t)} \mathcal{E}(t, \tau) \right\}, \quad (3)$$

where $\mathcal{F}_{t \rightarrow f}$ represents the Fourier transform from time t to frequency f , while $*_{(t)}$ represents a linear convolution in time t . This form uses the property that all time-frequency kernels can be related to the Fourier transform by yet another transform and this possesses practical advantages as the Fourier transform can be efficiently calculated using a FFT algorithm. However it should be emphasized that the time-frequency spectrum, called an evolutive spectrum, is

related to, but not equivalent to, a Fourier spectrum where the signal contains any significant non-stationary component.

The bilinear, cross power form \mathcal{C} is given by

$$\mathcal{C}(t, \tau) = z_1\left(t + \frac{\tau}{2}\right) z_2^*\left(t - \frac{\tau}{2}\right),$$

and the time-lag kernel function Φ is given by

$$\Phi(t, \tau) = \mathcal{F}_{\nu \rightarrow t}^{-1} \{f(\nu, \tau)\}.$$

Using discrete sequences, these equations may be re-expressed as follows,

$$\mathcal{S}(n, k) = 2 \sum_{m=L}^L \sum_{p=-L}^L \sum_{l=-L}^L e^{j2\pi(lp - km - ln/N)} \times f(l, m) z_1(p + m) z_2^*(p - m), \quad (4)$$

where $z = x + j\mathcal{H}(x)$ with x being a discrete time signal of odd length N , and $L = (N - 1)/2$.

Alternatively this may be put,

$$\mathcal{S}(n, k) = 2 \mathcal{F}_{m \rightarrow k} \left\{ \Phi(-n, m) * \mathcal{C}(n, m) \right\}, \quad (5)$$

where

$$\Phi(n, m) = N \mathcal{F}_{l \rightarrow n}^{-1} \{f(l, m)\}$$

is the discrete time time-lag kernel function, and

$$\mathcal{C}(n, m) = z_1(n + m) z_2^*(n - m)$$

is the discrete time bilinear product.

Table 1 shows the time-lag kernel functions for selected discrete time TFDs that we have tested for MT analysis, including the short-time Fourier transform (STFT) and the Cone kernel (CD) which are used here.

Table 1. Table of time-frequency kernels tested for MT processing.

Time-Frequency Representation	$\Phi(n, m)$
Periodogram (STFT) Flanagan, J.L. 1965; Portnoff 1981	$\begin{cases} \frac{1}{M} \Pi\left(\frac{n}{M-2 m }\right) & , m \leq \frac{M}{2} \\ 0 & , \text{otherwise} \end{cases}$
Wigner-Ville (WVD) Wigner 1932; Ville 1948	$\delta(n)$
Born-Jordan-Cohen (BJCD) Cohen 1966	$\frac{1}{2 m +1} \Pi\left(\frac{n}{2 m }\right)$
Choi-Williams (CWD) Choi and Williams 1989	$\begin{cases} \frac{\sqrt{\sigma\pi}}{2 m } e^{-\sigma n^2/4m^2} & , m \neq 0 \\ \delta(n) & , m = 0 \end{cases}$
Cone Kernel (CD) Zhao, Atlas and Marks 1990	$\begin{cases} e^{-2\alpha a^2} & , k \geq a n \\ 0 & , \text{otherwise} \end{cases}$

APPLICATION OF TIME-FREQUENCY DISTRIBUTIONS TO MT ANALYSIS

In practice, the calculation of the evolutive spectrum consists of using the chosen TFD to estimate the signal power spectrum in a window of an appropriate length (the greater the instability, the shorter the maximum window length), and then moving the window over the complete data record to obtain the temporal information. Within each window a spectral estimator, such as the Fourier transform, may then be applied. This spectral estimator is called the 'kernel' of the TFD. The spacing of successive windows depends on the desired balance between accuracy of estimation and speed of calculation. Obviously for the highest accuracy, a window spacing of one sample is best.

In using time-frequency analysis on MT broad-band noise data, we found that the TFDs are highly susceptible to stationary power leakage between the high and low frequencies. MT analysis is particularly susceptible to this problem since MT signals tend to contain much more power at low frequencies, so that the power leakage contaminates the high-frequency end of the spectra. The solutions we used to correct the leakage are analogous to those used in standard Fourier analysis. A taper was applied to the kernel window. This reduced leakage but did not entirely solve the problem, so we used interpolation in addition.

Interpolating within the window over which the kernel is to be applied is easily accomplished while forming the analytic signal. The analytic signal is essential to avoid the aliasing effect of the TFD kernels (without having to sample at twice the rate) which are based on a $\tau/2$ time support (Boashash 1988). The contrasts with the correlation kernel we are all familiar with from Fourier power spectral estimation which is based on a τ time support. The analytic signal is formed by taking its Fourier representation, doubling the estimates at positive harmonics and zeroing the estimates at negative harmonics without changing the zero frequency harmonic. Padding the Fourier representation with zeros produces the required kernel interpolation upon carrying out the inverse transformation. The unwanted interpolated frequencies, which contain the power leaked from the low-end spectral frequencies, are then rejected after the kernel calculation with minimal loss in power. This method was used for the CD distribution. This is not a totally adequate solution to the problem due to the power lost in the rejected interpolated frequencies, and leakage may still be serious for more violently varying signals.

Signal pre-whitening was also tried (Bendat & Piersol 1971, p. 332), however this was found to be more difficult to apply to TFDs than the interpolation procedure, so it was not used on this data. Because of the limitations of window size, time-frequency methods suffer from the problem of reduced-frequency bandwidth. To increase the bandwidth that we can analyse, we decimated the EMSLAB data using the appropriate anti-aliasing filter. The most convenient means of doing this for stationary data is to use Fourier methods to apply the filter and decimate. For non-stationary data a robust spectral estimator, such as the TFD, should be used instead of the Fourier transform. However, computing the inverse TFD is computationally intensive and has problems with phase matching. Therefore we used stationary Fourier decimation, checking the resultant signal

for introduced distortions. We found that we could safely decimate by four, but we were unable to achieve decimation by sixteen, as the results were too biased due to the non-stationarity in the increased bandwidth over which the 'decimation by sixteen' filter needed to operate.

The most obvious method of obtaining a site impedance estimate from the evolutive spectra is to determine the stationary signal spectra. A stationary signal component is constant across the signal so it can be extracted from the evolutive spectrum by statistical methods. The resultant stationary spectrum can then be analysed by normal MT analysis methods. However, this method was found to be very noisy as there did not seem to be any substantial stationary signal present in any of the data tested.

An alternative method of determining the site impedances is to calculate an impedance estimate for each time-frequency element. This gives an estimate of the instantaneous impedance for any spectral frequency at any time. The total impedance map can therefore be referred to as an 'evolutive impedance', just as a TFD spectrum is referred to as an evolutive spectrum. Since the impedance is a site function and is expected to be constant for the recording time, the instantaneous impedance estimates in any spectral frequency can be statistically reduced to a single impedance estimate equivalent to that produced by the stationary analysis of a stationary MT data set. Due to its robustness to non-normal distributions and outliers, the median was used to estimate the impedance amplitudes. The mode was used to estimate the phases, as the wrapping on the unit circle hides the wings of the distribution and even the median will generally result in biased estimates. We can therefore refer to this statistical estimate taken from the evolutive impedance distribution as a 'stationary impedance' estimate.

The statistical estimates were taken as the amplitude and phase rather than in the imaginary plane, as these are physically meaningful quantities. Though use of the phase introduces problems with unit-circle wrapping, there are obvious advantages in analysing a real physical property upon which physical constraints can be applied.

A useful technique for examining the validity of a stationary impedance estimate is to look at the scatter plot of the real part versus the imaginary part of the natural logarithm of the impedance. That is, the natural logarithm of the impedance amplitude and the linear impedance phase. The advantage of these plots is that the impedance amplitude and phase should now fall into normal, or at least peaked distributions which can easily be examined by eye for a central mode.

SELECTION OF A TIME-FREQUENCY KERNEL FOR MT ANALYSIS

The various time-frequency kernels from Table 1 were examined for suitability in the analysis of MT data. The instantaneous impedance scatter plots described previously were a useful tool for the empirical examination of these TFDs.

The TFD which is conceptually the closest to the standard Fourier transform is the STFT. The STFT assumes that a window width can be chosen over which the signal is locally stationary. Within this window a normal stationary Fourier

analysis can be applied. However, for broad-band signals, the STFT has the greatest smearing in time and frequency of all the TFDs. It also has a tendency to underestimate the power in highly non-stationary signals as seen in Fig. 1. The impedance scatter plots confirmed these findings (Fig. 5), especially in the case of the phase which had a uniform distribution and therefore gave no useful selection of a stationary impedance phase. The impedance amplitude distribution was much more scattered than that produced by any of the following TFDs.

One of the most popular TFDs is the Wigner-Ville Distribution (WVD), which satisfies many of the properties of a true energy distribution (Classen & Mecklenbräuker 1980). As can be seen from equation (6) the WVD is a form of time-frequency correlation function based on a $\tau/2$ lag step.

$$\mathcal{WVD}(t, f) = \int_{-\infty}^{\infty} z_1(t + \tau/2) \cdot z_2^*(t - \tau/2) e^{-j2\pi f\tau} d\tau. \quad (6)$$

The $\tau/2$ lag requires that the signal be sampled at two times the Nyquist rate and results in aliasing of the spectra when applied to real data sampled at the Nyquist rate. This is overcome, as stated previously, by the use of the analytic signal rather than the real signal.

A major problem with the use of the WVD is the large cross-terms (ghost signal) which develop between harmonics of the signal. The ghost signal is due to the bilinearity of the WVD kernel (Bouachache 1982) and is alternately positive and negative along the ghost component (Hudson 1974). For instance, a signal consisting of two chirps would have a ghost signal appearing symmetrically between the chirps on the frequency axis and with alternating signs in consecutive time windows. The WVD is therefore not totally suited to MT analysis since the presence of these terms tends to obscure features when the impedance curves are calculated. However, the alternating sign of the ghost terms, and the fact that MT signals tend to be a combination of many transient signals, means that these ghost terms will tend to cancel when statistical methods are used to isolate the stationary impedance. Useful results have been obtained from WVD analysis of MT data, especially where the signal approaches white noise, as is common with MT signals (Chant & Hastie 1990). In the case of the WVD, the impedance scatter plots showed considerable improvement in the amplitude distribution but no improvement in the phase distribution.

Variations on the WVD have been developed which use smoothing functions to reduce the magnitude of the cross-terms as well as general noise levels. This may be done by using a finite impulse response filter (FIR) in the time direction to take advantage of the alternating sign of the cross-terms. The smoothed WVD must be tailored to the signal, and in being smoothed, loses many of the useful attributes of the true TFD (Lovell 1991, p. 118).

Other TFDs address the problem of cross-terms by using time-frequency kernels which concentrate the energy of the ghost signal under the true signal components. The Born-Jordan-Cohen Distribution (BJCD) uses a kernel with a constant lag cross-section in the form of a uniform probability distribution function (Table 1). The kernel is independent of window length, so that the distribution

produces better results at medium window sizes, but gives no improvement for large window sizes and has problems with small windows. We have found this TFD useful for window lengths of 128 samples, but restrictive because it is generally desirable to work with a range of window sizes. The instantaneous impedance scatter plots gave impedance amplitude distributions as good as those of the WVD but also improved the phase distribution to the extent that reasonable estimates were obtained. However, at low spectral frequencies, where the periods are comparable to the window width, the distributions tended to break into two or more distinct distributions which makes estimation of the stationary impedance values difficult.

Another form of TFD we tested was the Choi-Williams Distribution (CWD). This has a kernel similar to that of the BJCD but adjusts itself to the window size. Another advantage of this distribution is the ability to control its smoothing function using the parameter σ . Varying σ controls the size of the cross-terms and the frequency resolution of the CWD. As σ is reduced the cross-terms diminish and are quite small for values of around 0.1, but resolution is reduced. As σ is increased, resolution is improved, but the cross-terms expand until at, $\sigma = 100$, the distribution approaches that of the WVD. A σ of between 1 and 10 has been recommended (Choi & Williams 1989), and in MT processing we found that $\sigma = 10$ gave adequate smoothing and sufficient resolution. In practice, we found that the CWD did not seem as effective at smaller window lengths (<128 samples) as the cone-shaped kernel. The CWD was found to have very good signal tracking and localization characteristics which were reflected in the instantaneous impedances. This tracking effect is useful for the identification of particular types of MT signal sources but makes statistical determination of a stationary impedance more difficult since the impedance distributions tend to be multimodal due to the variety of signal sources in any one MT data set.

The cone-shaped kernel distribution (CD) is one of the most recent kernels and has computational advantages over the CWD in that it has a constant lag cross-section. The smoothing factor α is chosen such that the kernel function $\Phi(n, m)$ is small at the extremities of the window. We found that choosing $e^{-2\alpha k} = 0.01$ at the extremities of the kernel produced good results. The standard value of 1 has been adopted for the parameter a which adjusts the slopes of the cone in the (t, τ) space (Table 1). The CD showed some of the signal tracking characteristics of the CWD but its signal localization was not as sharp. As a consequence, the instantaneous frequency distributions were more easily analysed for the stationary impedance estimate without too much complication by individual source effects. Though multiple distributions did appear, they were at lower spectral frequencies than with the BJCD, and the CD seemed to behave well with our broad-band MT data for all window lengths tested. Of the TFDs tested here, the CD TFD would appear to be the most useful of the TFDs for MT analysis.

In this paper we will use the STFT as one of our time-frequency analysis techniques because it compares most readily with the traditional Fourier techniques. Indeed a STFT with a quarter window overlap, or no overlap, is similar to the analysis used in some of the previous methods

(Jones *et al.* 1989; Thompson 1977). However the treatment of the resulting spectral estimations is quite different, since we do not use coherence as a weighting factor. The other TFD kernel we use is the CD, as we found that it is the most effective for our broad-band MT signals. Comparisons between these two TFDs will be made later in this paper which will show the superiority of the CD for broad-band MT analysis.

TIME-FREQUENCY ANALYSIS OF EMSLAB DATA

The MT data used in this analysis was kindly provided by Alan Jones (Jones *et al.* 1989). The data is a subset of that taken for site 1 of the EMSLAB electromagnetic survey of the Juan de Fuca area on the Lincoln Line sites, and has been used extensively to compare various MT processing techniques. Data was provided for times of 'active' and 'quiet' ionospheric activity, in order to compare the noise rejection properties of a processing technique. The results of conventional analysis of all the data taken at this site were made available so that a direct comparison might be made. To facilitate comparison with the other methods, apparent resistivities are compared in the unrotated form and impedances are calculated by the method outlined by Sims, Bostick & Smith (1971).

The method of analysis used here was to decimate the EMSLAB data by four using stationary decimation techniques. Time-frequency analysis was applied to each of the active and quiet period data sets and their decimations. The STFT was used to estimate the stationary impedances for comparison with the conventional methods of Fourier-based MT analysis. However, the statistics used were quite different to normal analysis methods. Of the TFDs the CD was chosen for the reasons given in the previous section. In both cases the Sims *et al.* (1971) method of calculating the impedance was used.

An analysis window length of 128 samples was used with a single sample period spacing between windows. The individual time-frequency impedance estimations were combined across time using a median filter on the impedance amplitudes and a mode selection on the phases. Processing from this point is identical to other methods with the unrotated apparent resistivities from the decimated and undecimated data being band-averaged into tenth-decade bands for comparison with the EMSLAB results.

TEMPORAL STABILITY OF THE IMPEDANCE TENSOR

Time-frequency analysis of MT data provides us with a time-varying estimation of the auto-powers and cross-powers for each frequency in the analysis. These spectra can be used to examine the behaviour of the impedance as a function of time and frequency by calculating the instantaneous impedance for each time-frequency power estimation. Using separate frequency elements from the evolutive impedance, we can examine the temporal stability of the impedance estimates.

According to standard MT theory, the time-dependent estimations of impedance made by time-frequency analysis of the signals should result in a constant impedance at each

frequency. That is, the impedance estimations should be distributed about a constant phase and amplitude for each frequency in a purely random manner. Figs 2 and 4 show examples of time-varying impedances taken at random from those produced during the analysis of the EMSLAB data. The impedance contains definite structure which is directly attributable to the various sources which dominate at different times.

The impedance makes smooth transitions between relatively stable estimates and highly biased estimates as the time window sweeps onto and past a non-stationary event (Fig. 2). We can examine the stationarity of signals which cause these excursions by correlation with the signal. This shows the biasing mechanisms to be non-stationary events and conclusively disproves the assumption that non-stationarity does not affect the impedance estimates.

Fig. 3 shows the same effects using STFT analysis. The basic non-stationary biases are visible under the increased noise level induced by the use of the Fourier transform kernel. This increased noise is due to the effect of less obvious non-stationary events and this is the reason we believe true TFD analysis necessary for the effective analysis of MT data. It should be obvious from Figs 2 and 3 that any statistical reduction to estimate a stationary impedance

value would give quite different results for the CD and STFT cases.

A biased impedance estimate can also be associated with a lack of signal as well as with the presence of a contaminating signal. This effect can be seen in the results shown in Fig. 7, where the lack of power in the quiet period data has resulted in biased apparent resistivity phase estimates at the lower spectral frequencies, in comparison to the active period shown in Fig. 9. Fig. 11 gives a comparison of the evolutive impedance distribution from a weak signal to that of a strong signal, showing the tendency to break into multiple distributions.

Figs 5 and 6 show scatter plots of the log of the impedance amplitude against the impedance phase for the STFT and CD respectively. Examination of both figures shows that the impedance amplitude estimates are log-normally distributed. This has particular implications for the statistical combination of multiple data sets, other than in the log domain. Any form of MT analysis based on linear normal statistics would give biased results and this will also affect the use of long-time Fourier methods which produce a linear mean of the signal over the record length. This is also true of weighted statistics based on coherences, since coherence calculations are based on the spectra which may be biased in

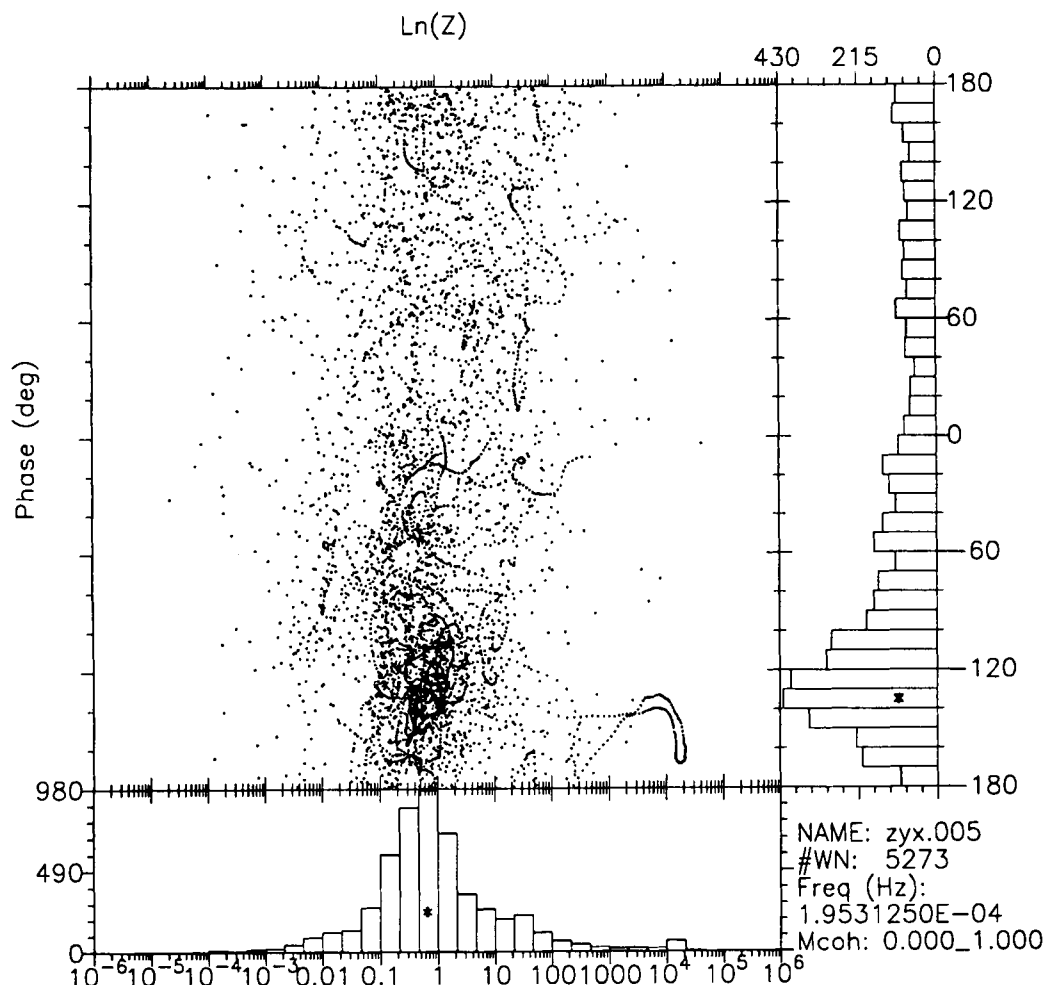


Figure 4. Plot of the log of a quiet period EMSLAB evolutive impedance amplitude against its phase at 1.95×10^{-4} Hz using the CD to derive the temporal variations in impedance. The plot shows considerable source-related structure.

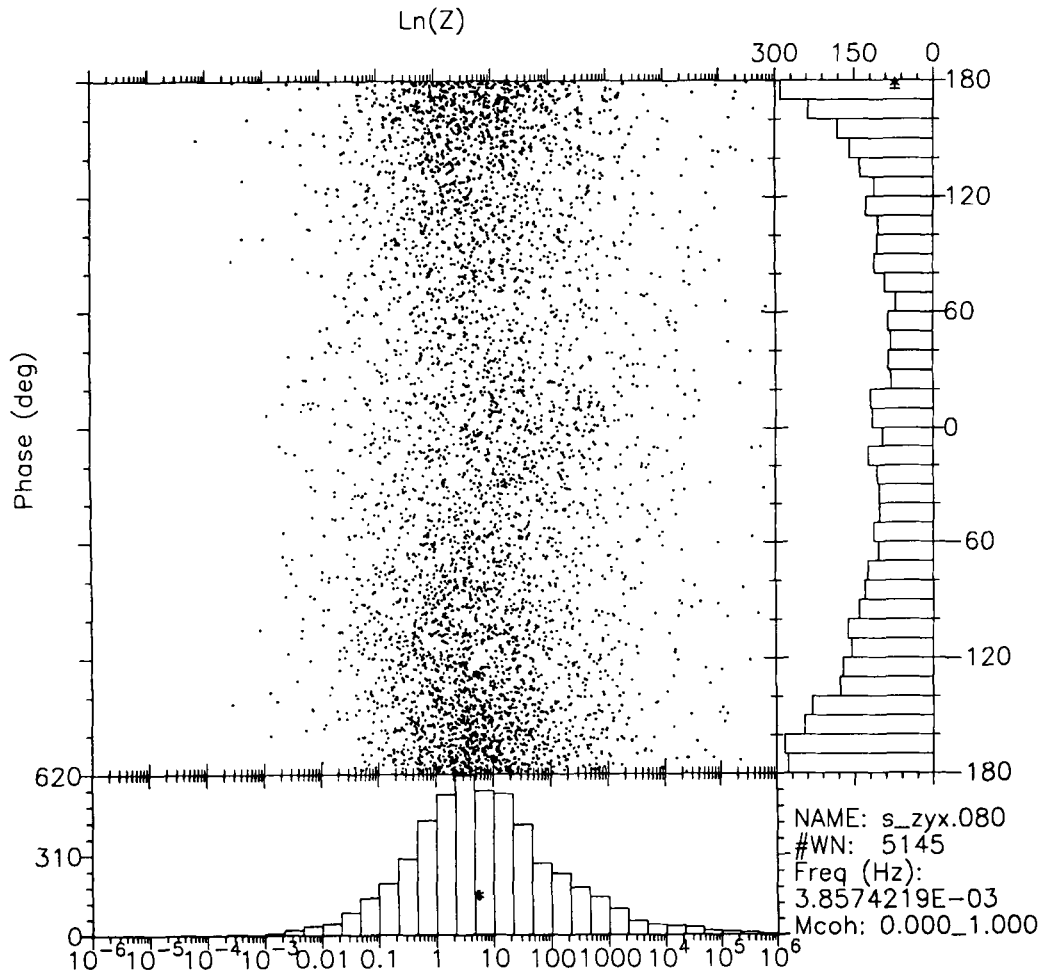


Figure 5. Plot of the log of a quiet period EMSLAB evulsive impedance amplitude against its phase at 3.86×10^{-4} Hz using the STFT to derive the temporal variations in impedance. The plot clearly shows the normally distributed log-amplitude structure and the highly scattered phase distribution.

the case of stationary analysis of non-stationary data. A robust statistic such as the median is effective at estimating the stationary impedance amplitude from the scatter plots in Figs 5 and 6.

Whereas the impedance amplitude falls into a normal distribution in log space, the phase distribution is normal in linear space but complicated by the wrapping effect on the unit circle. Therefore the tails of the phase distribution are not always evident and neither a mean nor a median will determine a good estimate of the peak value for phase. In this case, we must resort to an even more robust statistic and take the mode of the phase distribution.

One of the most striking features of Fig. 4 is the evidence of smooth variations which take place as the time window moves between dominant sources. It is quite evidently not a random fluctuation but a totally coherent signal which follows a distinct smooth path between dominant sources. These features are less evident in Figs 5 and 6 which are at higher spectral frequencies.

In time-frequency analysis of MT data we have a choice of using statistical methods on the time-frequency power spectral matrix or on the impedances developed from them. The advantage of working with the impedance, is that a

powerful signal (which gives stationary impedance estimates, but is only transiently present in the data) is not rejected. In using statistical filters to estimate the stationary component of the power spectra we are filtering out *all* non-stationary components of signal before we calculate the impedance. For the cases we have tried so far we have found that the character of the results obtained by either method was similar, but there was a major increase in noise for estimates based on statistical estimates of the power spectra due to a lack of a significant stationary signal component. We prefer the less noisy median of the evulsive impedances as it is both faster to calculate, and good impedance estimates associated with powerful transient MT signals are not rejected.

COMPARISON OF TIME-FREQUENCY METHODS

Figs 5 and 6 show comparative log-amplitude phase plots from the STFT and CD methods of time-frequency analysis. It is evident that the STFT has a much broader distribution than the CD. Indeed the evulsive impedance of Fig. 5 has poorly defined phase. The adverse effects of this broadening

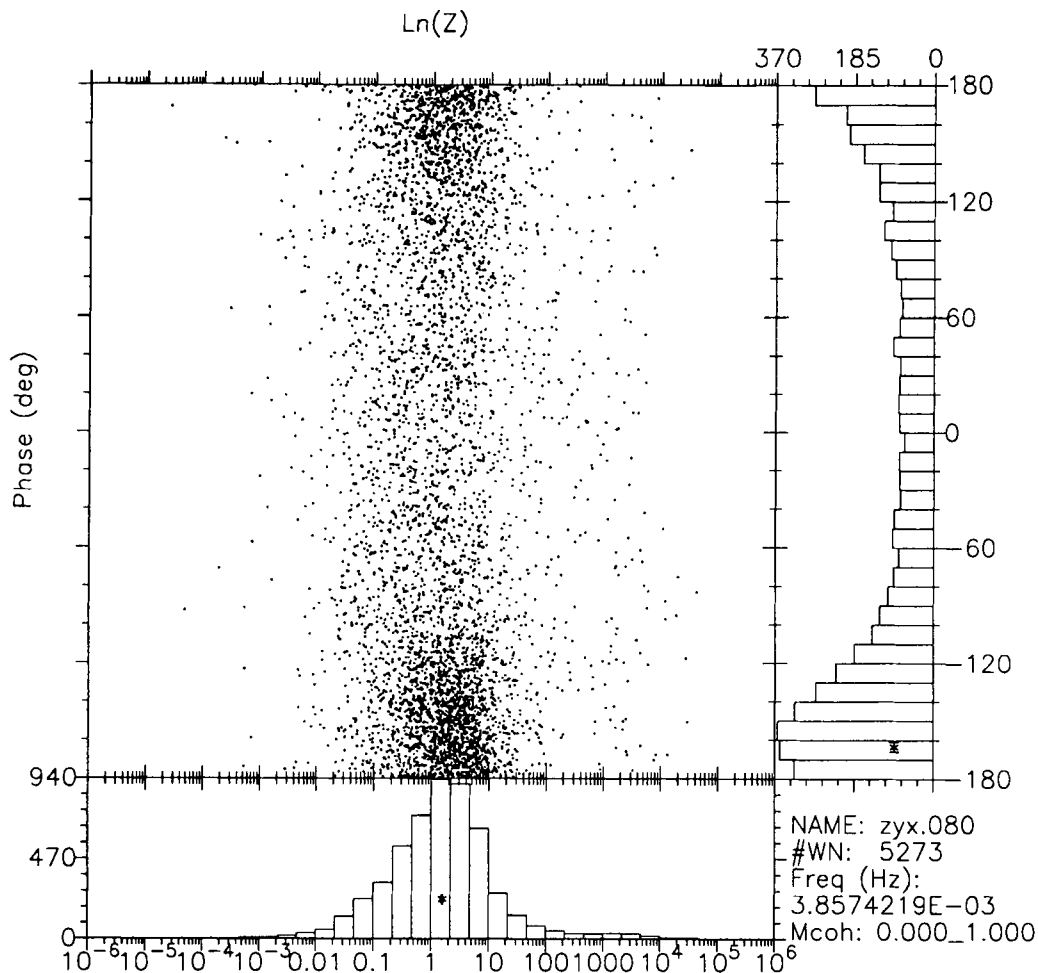


Figure 6. Plot of the log of a quiet period EMSLAB evulsive impedance amplitude against its phase at 3.86×10^{-4} Hz using the CD to derive the temporal variations in impedance. The plot clearly shows the normally distributed log-amplitude structure and the obviously peaked distribution of the phase. Notice that the log-amplitude distribution is more localized than for the STFT.

can be seen in the apparent resistivity and phase plots in Figs 7–10. This broadened distribution is a result of the poorer frequency resolution of the STFT and would also be symptomatic of the conventional ‘windowed’ MT processing methods. The problem can sometimes be reduced by careful selection of the window length, but this is not generally feasible with a broad-band noise signal such as MT signals.

COMPARISON WITH STANDARD EMSLAB RESULTS

A comparison of apparent resistivities and phases from time-frequency analysis is made with the conventional MT analysis of all data from site EMSLAB 1 as provided by Jones *et al.* (1989), in Figs 7–10. The STFT method shows reasonable agreement with the conventional data in all but the *E*-polarization apparent resistivities. In these the STFT is in much greater agreement with its *H*-polarization, indicating a far more one-dimensional structure than the conventional method. This disagreement is due primarily to the impedance components at each frequency having been estimated by the median of the evulsive impedances. Time-frequency phase estimates tend to agree with the

reference estimates as they are analysed by normal linear statistics in both methods. The time-frequency results are not as smoothed as the conventional results and the character of the curves is similar in both polarizations. The window overlap provides considerable smoothing along the time axis; however, the only smoothing along the frequency axis is provided by tenth-decade averaging used to match frequencies with the EMSLAB standard reference results.

The CD estimates in Figs 7–10 show even better agreement with the EMSLAB analysis on all but the *E*-polarization apparent resistivity amplitudes. These resistivity amplitudes are again similar to the *H*-polarization rather than to the reference *E*-polarization values, indicating a basically one-dimensional structure. The character of the curves in the *E* and *H*-polarization components are in fairly good agreement. Biases due to incoherent noise sources could still be present in these results as no effort has been made to remove this. The use of coherences to reject incoherent bias is difficult since no true coherence calculation is available for any TFD except the unsmoothed STFT (White 1989).

In Fig. 7 the CD phase estimates for the *E*-polarization of the quiet data below about 5×10^4 Hz depart radically from

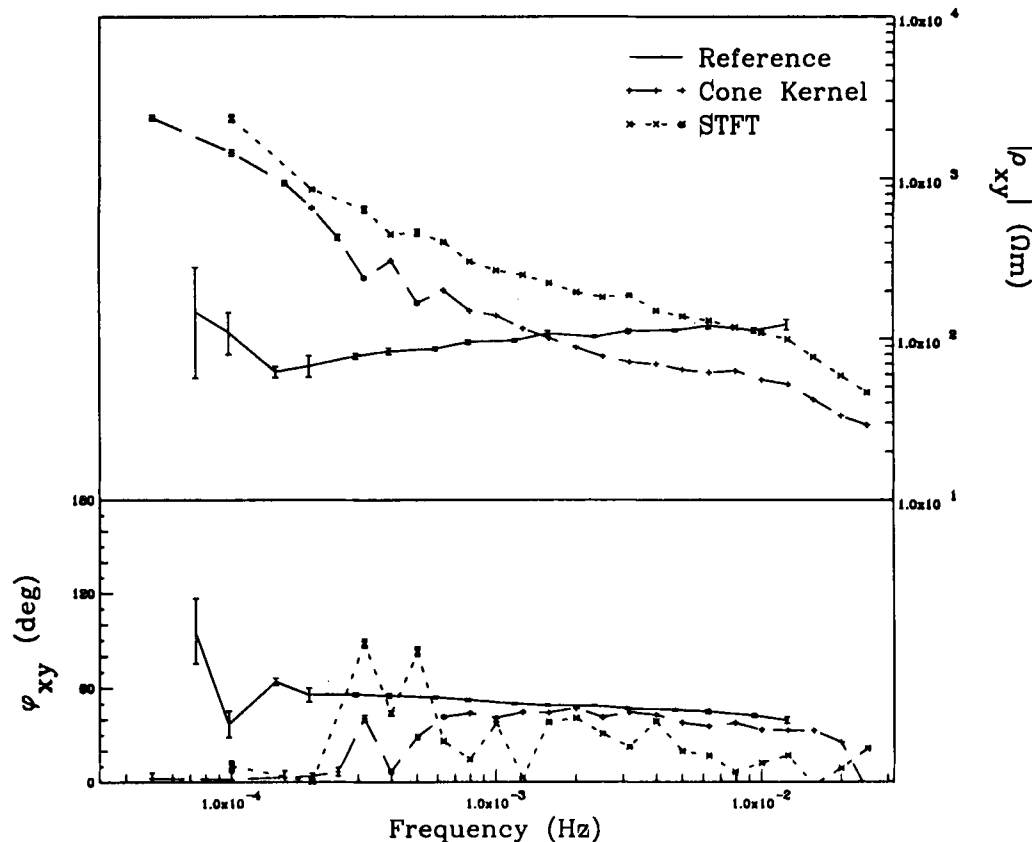


Figure 7. Apparent resistivity and phase plots of E -polarization for EMSLAB 1 quiet data using time-frequency analysis. Though the phase is similar to the reference data the amplitude is similar to the H -polarization and so is more consistent with a one-dimensional structure. Below 5×10^{-4} Hz the results suffer from lack of power. Errors are given on all points as one standard error of the median for the amplitude and of the mode for the phase.

the reference phases and from the CD phases in the active period. Examination of the apparent resistivity for the quiet and active periods for the E -polarization also shows a significant difference for these frequencies. Fig. 11 shows the log impedance versus impedance phase contour plot for one of these frequencies and for a higher frequency. The distribution at the higher frequency has an obvious central tendency whereas the estimate at the lower frequency is a multimodal distribution, indicating that only noisy, low-power signals were present at this time. The noisier estimates of the STFT suffer even more from this problem than the CD estimates, as seen in Figs 7–10. This problem indicates the need for some form of multimodal selection to be added to the stationarity selection already done. This also demonstrates the usefulness of the impedance distribution plots as a diagnostic tool.

Some of the MT processing methods detailed in Jones *et al.* (1989) have some of the attributes of the STFT. These methods, particularly the single-station robust approach (Egbert & Booker 1986), make an attempt to reject powerful transient non-stationary signals using robust statistics. However they do not address the total problem of non-stationarity nor the log normalcy of the impedance to estimations and will suffer from relatively poor amplitude and phase resolution in a similar manner to the STFT.

It should be noted that the results from the CD analysis

seem to indicate that the apparent two-dimensionality of the site may be largely a function of the difference in signal-to-noise ratio in the two directions. It would be expected that in MT data this type of effect might not be uncommon.

RECOMMENDED ACQUISITION TECHNIQUES FOR USE WITH TIME-FREQUENCY MT ANALYSIS

In the light of these developments in time-frequency MT analysis, certain recommendations can be made as to the way data is acquired in exploration field surveys that would facilitate time-frequency MT analysis. For time-frequency analysis there are distinct advantages in acquiring and processing a single contiguous data set. Because of the nature of non-stationary signals, separate data sets may have local stationarity which will give an erroneous value of impedance. By analysing a contiguous length the problem of local stationarity is greatly reduced. A multimodal detection system could be used on the evolutive impedances of each frequency to determine when enough data had been acquired for firm unimodal impedance estimates. With the introduction of a non-stationary decimation filter this would allow a large data set to provide wide bandwidth information on a site.

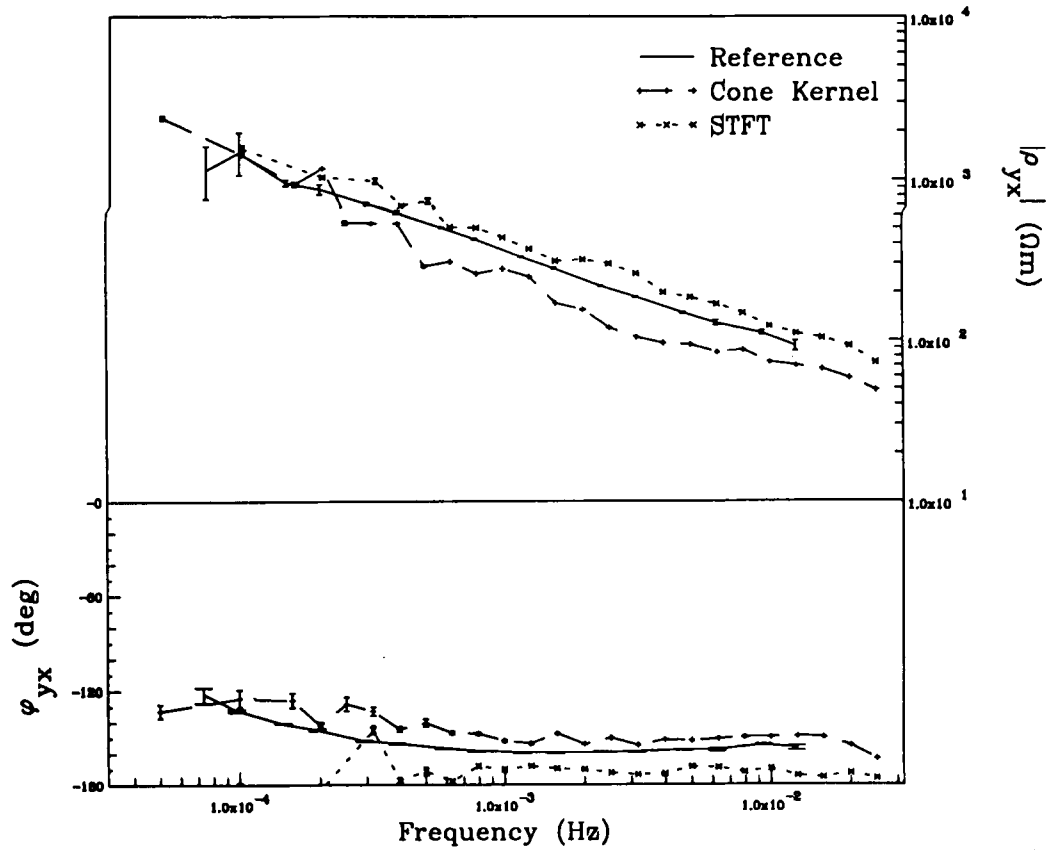


Figure 8. Apparent resistivity and phase of the H -polarization for EMSLAB 1 quiet data using time-frequency analysis. The results are consistent with the reference. Errors are given on all points as one standard error of the median for the amplitude and mode for the phase.

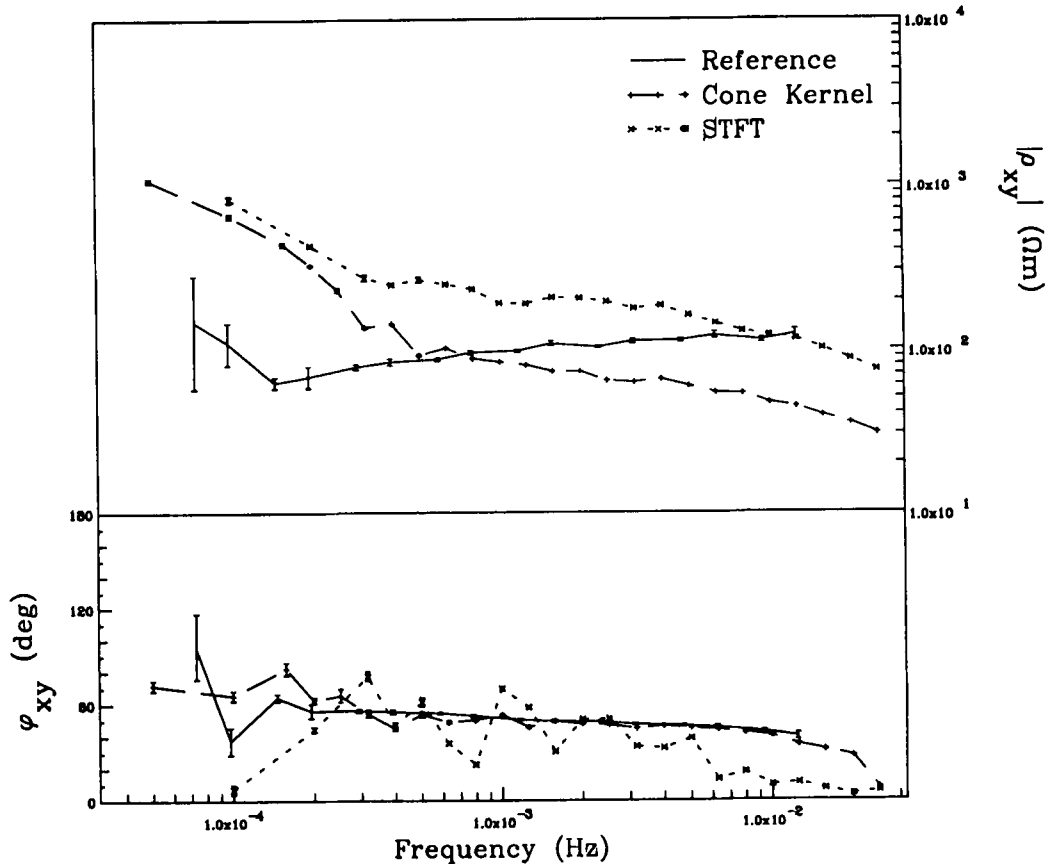


Figure 9. Apparent resistivity and phase plots of E -polarization for EMSLAB 1 active data using time-frequency analysis. Results are consistent with the 'quiet' data results but with sufficient power below 5×10^{-4} Hz for reasonable resolution, especially using the CD. Errors are given on all points as one standard error of the median for the amplitude and mode for the phase.

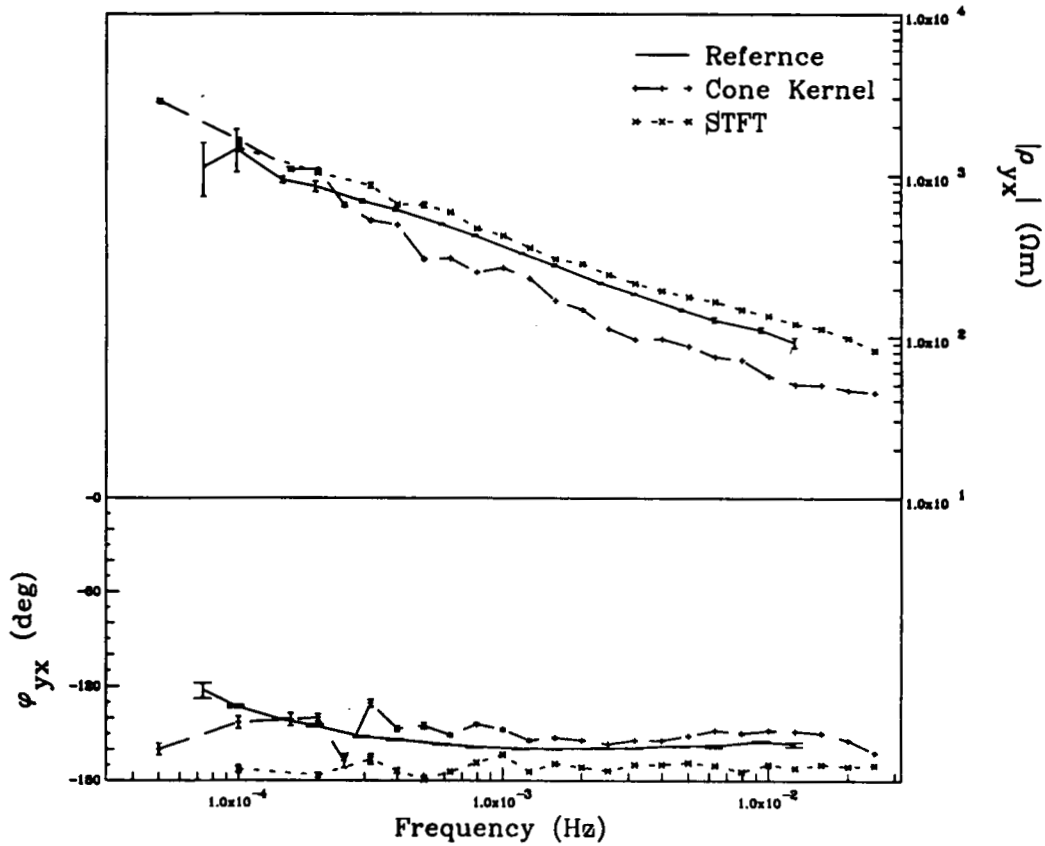


Figure 10. Apparent resistivity and phase plots of H -polarization for EMSLAB 1 active data using time-frequency analysis. Results are consistent with the 'quiet' period results. Errors are given on all points as one standard error of the median for the amplitude and mode for the phase.

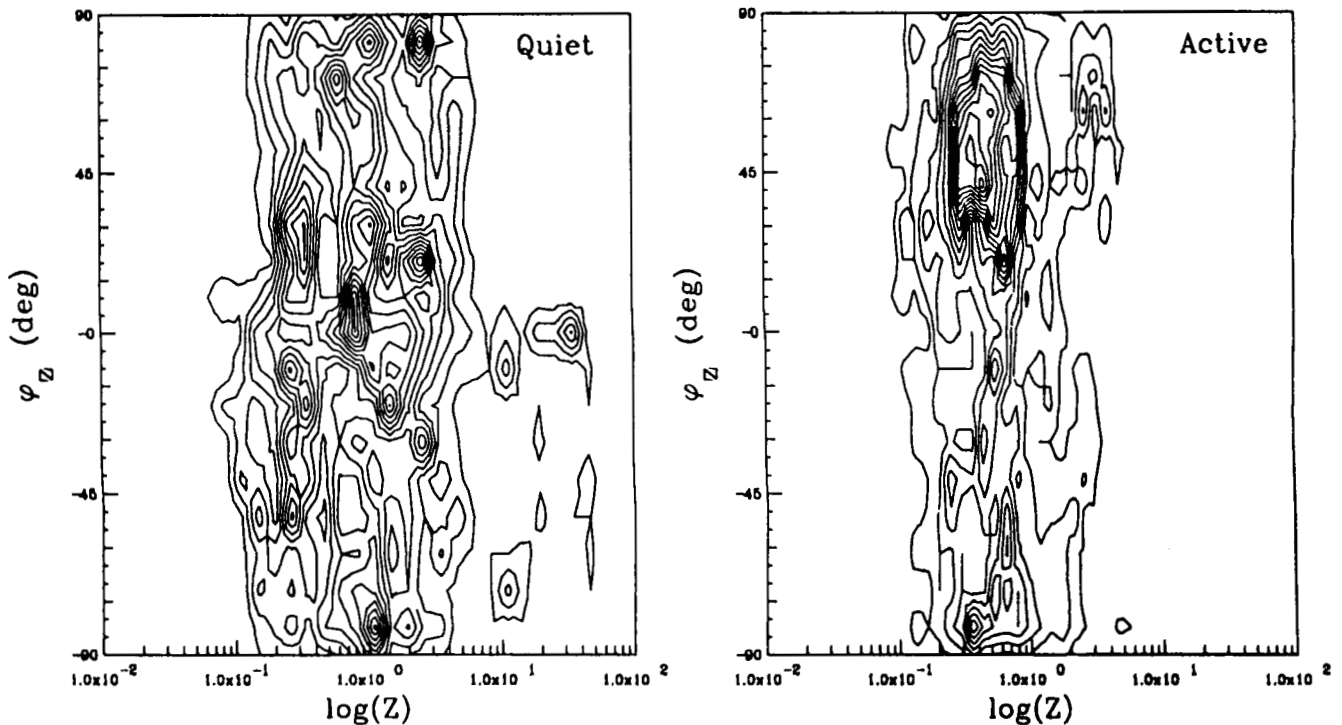


Figure 11. Contour plots of the log impedance versus impedance phase distributions (Z_{xy}) for a quiet (1.46×10^{-4} Hz) and an active (4.39×10^{-4} Hz) period using the CD. The quiet period results exhibit multiple modes between which we are unable to discriminate effectively. This indicates the need for another selection criterion (perhaps coherence) in addition to stationarity selection.

FUTURE WORK

A number of improvements and extensions to our work on time-frequency analysis of MT data are planned or underway. These include improved filtering techniques for the estimation of the stationary impedance, and examination of time-frequency coherence estimators and their application to mode selection in a multimodal signal. Some work has already been done to compare time-frequency analysed MT with CSAMT results at a site (Chant & Hastie 1991). This work used only the Wigner–Ville distribution and will be extended to the newer TFD kernels in the immediate future. A time-frequency examination of the polarization ellipses of the signal sources may provide further information on source discrimination. To facilitate the use of time-frequency analysis on MT signals further work is needed on time-frequency decimation filtering.

CONCLUSIONS

This paper has clearly demonstrated the following important points.

- (1) MT signals due to natural sources are generally highly non-stationary.
- (2) MT impedance estimates are strongly affected by the non-stationarities in the electromagnetic fields.
- (3) Due to point 2, MT impedance estimates made using spectral estimates based stationary signal processing methods, such as the Fourier transform, are generally biased and noisy.
- (4) The proposed time-frequency method of estimating the impedances using time-frequency distributions (TFDs) to produce an evolutive impedance estimate offers a reasonable procedure for minimizing the non-stationary bias, as well as providing a good basis for further studies of data quality and source structure.

The use of stationary based coherence estimates as a primary selection criterion for weighting MT data is seen as a highly questionable approach. This is because the coherence estimates are based on biased spectral representations derived from stationary methods. Of the TFDs we tested, we found the cone distribution (CD) most effective in broad-band MT processing, and better at resolving the stationary signal than the short-time Fourier transform (STFT), which is less robust to non-stationarity.

REFERENCES

- Bendat, J. S. & Piersol, A. G., 1971. *Random Data, Analysis and Measurement Procedures*, Wiley, New York.
- Berdichevski, M. N., 1960. Principles of magnetotelluric profiling theory, *Appl. Geophys.*, **28**, 70–91.
- Berdichevski, M. N., 1964. Linear relationships in the magnetotelluric field, *Appl. Geophys.*, **38**, 99–108.
- Boashash, B., 1988. Note on the use of the Wigner distribution for time-frequency analysis, *IEEE Trans. Acoustic. Speech Signal Process.*, **36**, 1518–1521.
- Boashash, B., 1991. *Advances in Spectral Estimation and Array Processing, Part I*, ch. 9, Prentice-Hall, Englewood Cliffs, N.J.
- Bouachache, B., 1982. Representation temps-frequence, *PhD thesis*, Inst. Nat. Polytechnique, University of Grenoble (France).

- Chant, I. J. & Hastie, L. M., 1990. The Wigner–Ville analysis of magnetotelluric signals, *Proceedings Geological Soc. of Australia*, No. 25, pp. 89–90.
- Chant, I. J. & Hastie, L. M., 1991. A comparison of Fourier and Wigner–Ville signal processing methods applied to a magnetotelluric survey of the Kenmore oil field, *Proceedings Australian Society of Exploration Geophysicists 8th Conference & Exhibition & Geological Society of Australia Exploration Symposium*, pp. 42–43.
- Chave, A. D. & Thomson, D. J., 1989. Some comments on magnetotelluric response functions estimation, *J. geophys. Res.*, **94**, 14 201–14 213.
- Chave, A. D., Thomson, D. J. & Ander, M. E., 1987. Robust estimation of geomagnetic transfer functions, *J. geophys. Res.*, **92**, 633–648.
- Choi, H. & Williams, W. J., 1989. Improved time-frequency representation of multicomponent signals using exponential kernels, *IEEE Trans. Acoustic. Speech Signal Process.*, **37**, 862–871.
- Classen, T. A. C. M. & Mecklenbräuer, W. F. G., 1980. The Wigner distribution—a tool for time-frequency analysis, Part I. Continuous-time signals, *Phillips J. Res.*, **35**, 217–250.
- Cohen, L., 1967. Generalized phase space distributions, *J. math. Phys.*, **7**, 181–186.
- Dekker, D. L. & Hastie, L. M., 1981. Sources of error and bias in a magnetotelluric depth sounding of the Bowen Basin, *Phys. Earth planet Inter.*, **25**, 219–225.
- Egbert, G. D. & Booker, J. R., 1986. Robust estimation of geomagnetic transfer functions, *Geophys. J. R. astr. Soc.*, **87**, 173–194.
- Flanagan, J. L., 1965. *Speech Analysis: Synthesis and Perception*, Springer Verlag, Berlin, NY.
- Goubau, W. M., Gamble, T. D. & Clarke, J., 1978. Magnetotelluric data analysis: removal of bias, *Geophysics*, **43**, 1157–1166.
- Hudson, R. L., 1974. When is the Wigner quasi-probability density non-negative, *Reports on Mathematical Physics*, **6**, 249–252.
- Jones, A. G., 1981. Transformed coherence functions for multivariate studies, *IEEE Trans. Acoust. Speech Signal Process.*, ASSP-29, 317–319.
- Jones, A. G. & Jödicke, H., 1984. Magnetotelluric transfer function estimation improvement by coherence based rejection techniques, *Presented by Soc. of Expl. Geophys., 54th International Meeting*.
- Jones, A. G., Chave, A. D., Egbert, G., Auld, D. & Bahr, K., 1989. A comparison of techniques for magnetotelluric response function estimation, *J. geophys. Res.*, **94**, 14 201–14 213.
- Lovell, B. C., 1991. Techniques for nonstationary spectral analysis, *PhD thesis*, University of Queensland.
- Pornoff, M. R., 1981. Time-scale modifications of speech based on short-time Fourier analysis, *IEEE Trans. Acoust. Speech Signal Process.*, ASSP-29, 374–390.
- Reddy, I. K. & Rankin, D., 1975. Magnetotelluric response of laterally inhomogeneous and anisotropic media, *Geophysics*, **40**, 1035–1045.
- Sims, W. E., Bostick, F. X. & Smith, H. W., 1971. The estimation of magnetotelluric impedance tensor elements from measured data, *Geophysics*, **36**, 938–962.
- Soong, T. T., 1981. *Probabilistic Modeling and Analysis in Science and Engineering*, Wiley & Sons, New York.
- Thomson, D. J., 1977. Spectrum estimation techniques for characterization and development of the WT4 waveguide, *1, Bell. Syst. tech. J.*, **56**, 1769–1815.
- Tikhonov, A. N. & Berdichevski, M. N., 1966. Experience in the use of magnetotelluric methods to study the geological structures of sedimentary basins, *Izv. Phys. Solid Earth*, **2**, 34–41.

- Ville, J., 1948. Théorie et applications de la notion de signal analytique, *Cables et Transmissions*, **2**, 61–74.
- Vozoff, K., 1972. The magnetotelluric method in the exploration of sedimentary basins, *Geophysics*, **37**, 98–141.
- White, L. B., 1989. Some aspects of time-frequency analysis of random processes, *PhD thesis*, University of Queensland, Queensland, Australia.
- Wigner, E. P., 1932. On the quantum correction for thermodynamic equilibrium, *Phys. Rev.*, **40**, 749–759.
- Zhao, Y., Atlas, L. E. & Marks, R. J., 1990. The use of cone-shaped kernels for generalized time-frequency representations of non-stationary signals, *IEEE Trans. Acoustic. Speech Signal Process*, **38**, 1084–1091.